New mouse model of cholangiocarcinoma arising in the setting of progressive biliary injury and fibrosis

Pinzhu Huang[1], Guangyan Wei [1], Shuangshuang Zhao[1], Disha Badlani[1], Kahini Vaid[1], Li Chen[2], Mathieu Petitjean[2], Xin Chen[3], Gregory Gores[4], Yury Popov[1#]

[1]Beth Israel Deaconess Medical Center, Harvard Medical School, Boston, MA; [2]PharmaNest, Inc; [3]University of California, san Francisco, CA and [4]Division of Gastroenterology and Hepatology, Mayo Clinic, Rochester, MN (*[#]contact: ypopov@bidmc.harvard.edu*)

BACKGROUND & AIMS: Cholangiocarcinoma (CCA) is a dreaded complication of primary sclerosing cholangitis (PSC), difficult to diagnose and associated with high mortality. Lack of high-fidelity animal models of CCA that recapitulate the hepatic microenvironment of progressive sclerosing cholangitis precluded basic studies into the underlying mechanisms and development of effective treatment. Here, we report the establishment and characterization of a mouse model of PSC-associated CCA.

METHODS: Ten weeks old Mdr2-/- mice with congenital PSC-like progressive biliary disease, and healthy wild-type littermates (WT) mice were subjected to either modified retrograde biliary instillation (*Yamada, et al. Hepatology 2015*, without concomitant IL-33 or bile duct ligation) or hydrodynamic tail vein injection (*Zhang, et al. J Hepatol 2017*) of sleeping beauty transposon-transposase plasmid system with activated forms of AKT (myr-AKT) and Yap (YapS127A) protooncogenes (SB AKT/YAP1). ALK5 inhibitor (SB-525334, 300 mg/kg in diet) or placebo diet was administered into tumor-bearing mice starting from 1 week post-oncogene transduction to interrogate functional role of TGFβ signaling in our model. Tumor phenotype and burden were analyzed using histological methods. Desmoplastic stroma of the tumors was characterized and quantified using automatic FibroNest platform (PharmaNest Inc) from Picrosirius Red (PSR) staining.

RESULTS: While SB AKT/YAP1 plasmids via retrograde biliary injection caused tumors in all Mdr2-/- but not in healthy wildtype mice (n=10), only 26.67% (4/15) of these tumors were CCA and this approach was deemed unsuccessful (**Figure 1A-B**). Alternative, hydrodynamic tail vein injection of SB AKT/YAP1 resulted in robust tumorigenesis in fibrotic female Mdr2-/- mice (n=10), with 100% incidence and high CCA burden after 6 weeks. In contrast, only 6 out of 9 healthy wildtype mice (66.67% incidence) developed tumors. Higher CCA numbers (52.60±6.81 vs.1.11±0.51, p<0.01) with significantly shortened survival were observed in Mdr2-/- mice compared to non-fibrotic controls (**Figure 1C-E**). Similar to female mice, male Mdr2-/- mice also presented significantly higher tumor burden than WT mice (**Figure 1F-H**). CCA in Mdr2-/- mice exhibited desmoplastic reaction and were positive for Ki67, CK19, Sox9, α-SMA and TGFβ1, but negative for HNF4α and glutamine synthetase, and weak for CD31. Magnification, x200. Scale bar: 50 μm. (**Figure 2**). Early pharmacological TGFβ inhibition via ALK5 reduced tumor burden by 2.4 fold (11.00±1.41 vs. 24.80±5.75, n=5, p=0.0481) and desmoplastic stroma indicated by assemble collagen area, collagen fiber density of the tumors compared to placebo (**Figure 3**).

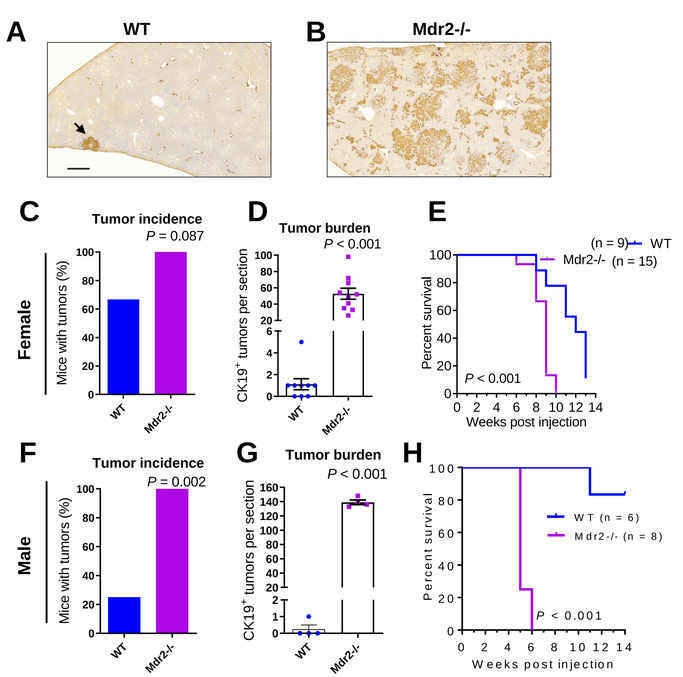

Figure 1. Tumorigenesis in wildtype and Mdr2-/- mice with hydrodynamic tail vein injection of AKT/YAP1 SB transposon-transposase. (**A**) Representative CK19 staining images of livers in WT (left) and fibrotic Mdr2-/- (right) mice with transduction of AKT/YAP1. Magnification x20, scale bar: 500 μm. (**B-H**) Quantifications of tumor incidence, microscopic tumor numbers, and survival curves of WT and Mdr2-/- mice. p value was determined by Chi-square test for incidence, unpaired two-tailed t test for tumor number and log rank test for survival.

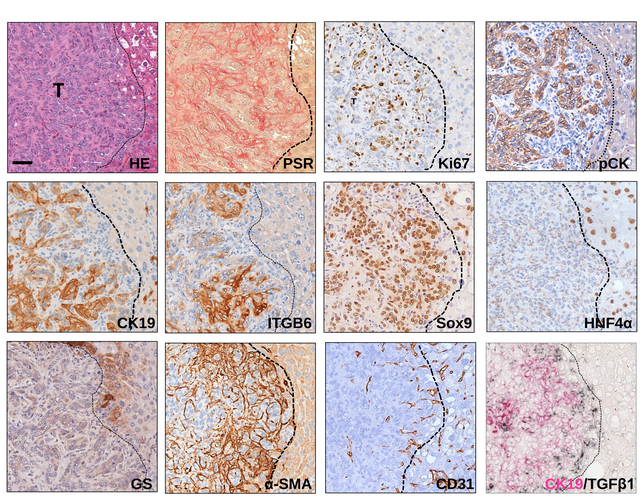

Figure 2. Phenotypic characterization of the tumors arising in mice with hydrodynamic tail vein injection of AKT/YAP1/ SB transposon-transposase. All tumors were defined as cholangiocarcinoma (CCA) characterized by atypical cells forming tubular structures (H&E) with pronounced desmoplastic reaction (Picrosirius Red). Tumors are uniformly positive for Ki67, pCK CK19, Sox9, α-SMA, TGF**β1,** negative for HNF4α and glutamine synthetase, weak for CD31. ITGB6 is variously expressed in tumor. Magnification, x200. Scale bar: 50 μm.

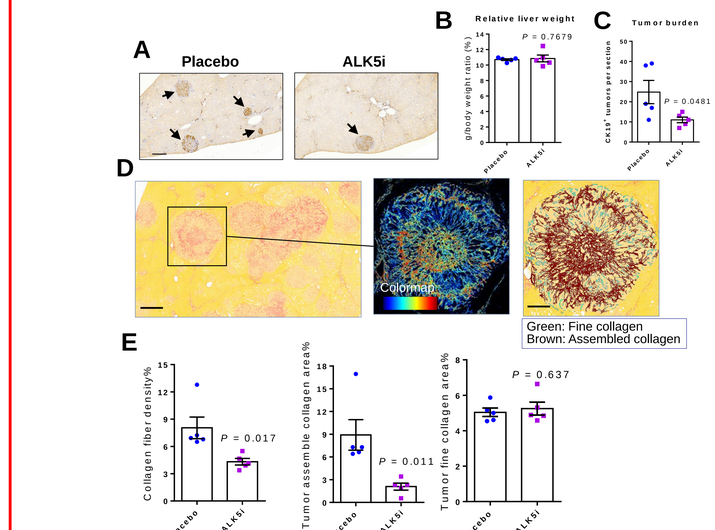

Figure 3. The effect of ALK5 inhibition on tumor progression of SB CCA.Mdr2-/- model at 1-4 weeks post injection. (A) Representative CK19 staining images of livers (Magnification x20, scale bar: 500 μm). Arrows indicate visible tumor nodules. (B) Relative liver weight and (C) CK19+ tumor number. (D) Representative images of desmoplastic tumor tissue (picrosirius red, magnification x20 , scale bar: 500 μm) (left panel). Color map (middle panel, with higher colors showing higher collagen density) and fibrosis phenotype (right panel) (magnification x50, scale bar: 200 μm). (E) Intratumorally collagen architecture was analyzed for collagen fiber density, assembled and fine collagen area (unpaired two-tailed t test).

CONCLUSIONS:

We established a new high-fidelity cholangiocarcinoma model in mouse, termed SB CCA.Mdr2-/-. It recapitulates the increased susceptibility to CCA in the setting of progressive biliary injury and fibrosis observed in PSC, and enables mechanistic research and formal testing of new therapies for this devastating disease. Furthermore, pharmacological targeting of Alk5 in our model suggests that TGFb signaling functionally drives CCA tumorigenesis and promotes desmoplastic reaction in a complex, stage-specific manner.